Modeling Alpine Grassland Above Ground Biomass Based on Remote Sensing Data and Machine Learning Algorithm: A Case Study in East of the Tibetan Plateau, China

Baoping Meng, Tiangang Liang, Shuhua Yi, Jianpeng Yin, Xia Cui, Jing Ge, Mengjing Hou, Yanyan Lv, and Yi Sun

***Abstract*—Effective and accurate assessment of grassland aboveground biomass (AGB) especially via remote sensing (RS), is crucial for forage-livestock balance and ecological environment protection of alpine grasslands. Because of complexity and extensive spatial distribution of natural grassland resources, the RS estimation models based on moderate resolution imaging spectroradiometer (MODIS) data exhibited low accuracy and poor stability. In this study, various methods for estimating the AGB of alpine grassland vegetation using MODIS vegetation indices were evaluated by combining with meteorology, soil, topography geography and *in situ* measured AGB data (during grassland growing season from 2011 to 2016) in Gannan region. Results show that 1) five out of ten factors (elevation, slope, aspect, topographic position, temperature, precipitation and the concentration of clay and sand in the soil) exert significant effects on grassland AGB, with R^2 0.04–0.39, and RMSE 859.68–1075.09 kg/ha, respectively; 2) the accuracy and stability of AGB estimation model can be improved by constructing multivariate models, especially using multivariate nonparameter models; 3) the optimum estimation model is constructed on the basis of random forest algorithm (RF). Compared with univariate/multivariate parameter models, RMSE of RF model decreased 26.45%–44.27%. Meanwhile, RF models can explain 89.41% variation in AGB during grass growing season. This study presented a more suitable RS inversion model integrated MODIS vegetation indices and other effect factors. Besides, the accuracy based on MODIS data was greatly improved. Thus, our study provides a scientific basis for effective and accurate estimating alpine grassland AGB.**

Manuscript received March 21, 2020; revised May 14, 2020; accepted May 25, 2020. Date of publication June 2, 2020; date of current version June 16, 2020. This work was supported in part by the National Key Research and Development Program of China project under Grant 2017YFA0604801 and Grant 2017YFC0504801, in part by the National Natural Science Foundation of China Grant 31672484, Grant 41401472, and Grant 31901393, and in part by the Fundamental Research Funds for the Central Universities under Grant lzujbky-2019-93. *(Corresponding authors: Tiangang Liang; Shuhua Yi.)*

Baoping Meng, Shuhua Yi, Yanyan Lv, and Yi Sun are with the Institute of Fragile Eco-environment, School of Geographic Science, Nantong University, Nantong 226007, China (e-mail: mengbp09@lzu.edu.cn; yis@ntu.edu.cn; lvyy09@lzu.edu.cn; sunyi@ntu.edu.cn).

Tiangang Liang, Jianpeng Yin, Jing Ge, and Mengjing Hou are with the State Key Laboratory of Grassland Agro-Ecosystems, College of Pastoral Agriculture Science and Technology, Lanzhou University, Lanzhou 730000, China (e-mail: tgliang@lzu.edu.cn; yinjp17@lzu.edu.cn; gej12@lzu.edu.cn; houmj17@lzu.edu.cn).

Xia Cui is with the Key Laboratory of Western China's Environmental Systems (Ministry of Education), College of Earth and Environmental Sciences, Lanzhou University, Lanzhou 730000, China (e-mail: xiacui@lzu.edu.cn).

Digital Object Identifier 10.1109/JSTARS.2020.2999348

***Index Terms*—Above ground biomass (AGB), alpine grassland, machine learning algorithm, multivariate model.**

I. Introduction

GRASSLAND ecosystem, as the largest terrestrial ecosystem on earth's surface [1], accounts for about 40% of land area [2], its net primary productivity accounts for 20% of the total terrestrial ecosystem capacity [3]. Above ground biomass (AGB), usually expressed as dry grass weight of aboveground portion within one unit area [4], is an important indicator of regional carbon cycle [5], [6]. Its temporal and spatial patterns reflect carbon sink potential of grassland vegetation [7], [8]. In addition, grassland AGB and its change directly reflect degree of grassland degradation, soil erosion [9]–[11], and desertification [12]. In practice, changes in grassland AGB can be used to monitor pasture overgrazing and land use change [13]. Therefore, accurate estimation of grassland AGB is of great significance for grassland management, grass and livestock balance, grassland growth assessment, and ecological environmental protection [14]–[16].

Ground measurement and remote sensing (RS) inversion are two major methods in grassland AGB estimation. RS inversion methods have gradually replaced traditional ground measurement methods, and showed more application possibilities with significant advantage of macroscopic, rapid, economical, and informative information [17]. RS inversion has become the most effective method for collecting continuous spatial and temporal data at regional or even global scales [18]–[23].

Normalized vegetation index (NDVI) was first applied to study natural grasslands in the early 1970s, seemingly, research on the linkage between vegetation indices and AGB had a history extending over several decades [24], [25]. For example, Li and Liu estimated wetland vegetation biomass based on Landsat ETM NDVI and field sampling data in Poyang Lake, the correlation between biomass and NDVI showed high coefficient of 0.80 [26]. Xu *et al.* constructed grassland AGB inversion model based on MODIS NDVI and field measurement data in the Tibetan Plateau from the end of July to September in 2007 [27]. Cui *et al.* used MODIS NDVI at 500 m resolution to construct AGB regression model for the alpine meadow grassland [21].

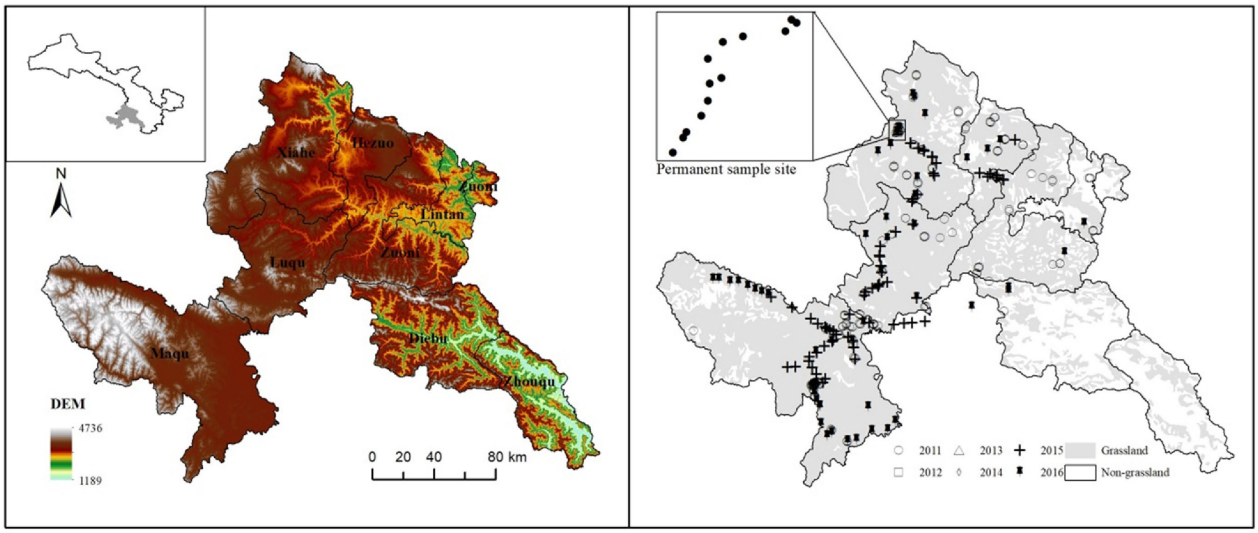

(a) (b)

Fig. 1. (a) Location of study area and (b) distribution of sampling sites in the pastoral area of Gannan region, China. Black spots in Fig. 1(b) represent location of permanent sampling sites, other symbols represent random sampling sites, each sampling site corresponded to one MODIS pixel, and the growth status of grassland was relatively uniform.

High-resolution satellite image such as MSS, TM, and SPOT, has been used in grassland AGB monitoring in several studies exhibited higher accuracy, but it is severely constrained by several factors such as passing time, coverage, and cloud rain. Although MODIS has a low spatial resolution, it has a high temporal resolution (every day) and a large spatial coverage (width of 2330 km). Those features are suitable for monitoring of grassland AGB and its dynamic changes especially for large areas [24]. However, univariate parameter RS inversion models based on MODIS data have low accuracy and poor stability in alpine meadow grassland [23], [28], [29], because of the extensive spatial distribution, complex grass species, and high spatial heterogeneity [14], [29], [24]. Hence, it is essential to explore a new grassland AGB monitoring method based on MODIS data. Quan *et al.* improved the accuracy of AGB estimation by using PROSAILH radioactive transfer model, with R^2 increased by 0.16 than empirical statistical models [30]. He *et al.* presented a physical method based on assimilate data retrieved from MODIS to improve the AGB estimation accuracy [31]. Ali *et al.* analyzed applicability of multiple linear regression (MLR), artificial neural network (ANN), adaptive neuro-fuzzy inference system (ANFIS) models, results showed that ANFIS has produced improved estimation of biomass as compared to the ANN and MLR [32]. Furthermore, additional critical factors like topographic, meteorological, soil and vegetation biophysical indicators are taken into construction of RS inversion model [20], [22], [24], [27], [29], [33]–[36]. Various form and structure of RS estimation models have been applied in AGB estimation study, i.e., multivariate parameter models include linear, logarithmic, power and reciprocal formula forms [23], [34], [35], multivariate nonparameter models include back propagation artificial neural network (BP-ANN), support vector machine (SVM), random forest (RF) [20], [36]–[40], and so on.

In this study, the major aims are as follows:

1) examine the critical factors (meteorology, soil, topography, geography and remote sensing vegetation indices) in estimating AGB of alpine meadow;
2) compare and analyze the performance of three types of AGB estimation models (univariate parameter models, multivariate parameter and multivariate nonparameter models) in alpine meadow;
3) propose a method with easy-operation and high accuracy for alpine grassland AGB estimation.

Based on the above results, this study will provide scientific support for high-precision remote sensing inversion of large-scale grassland AGB.

II. Methods and Materials

A. Study Area

Gannan region (33°60′–35°44′ N, 100°46′–104°44′ E) is one of the important agricultural and pastoral intersections in the northeastern Qinghai-Tibet Plateau (see Fig. 1), located on the transition zone of Loess Plateau to the Tibetan Plateau. Mean elevation is greater than 3000 m. As its vast area (account for 70.28% of the total area), livestock grazing is the primary activity in this region and closely related to human well-being. This region has a continental plateau climate: mean annual air temperature ranges from 1 to 3 °C, annual precipitation varies from 400 to 800 mm, and annual mean sunshine duration is 2000–2400 h. Rain and heat are concentrated in June to August, which are peak period of grassland growth. The main grassland types are alpine meadow and alpine shrub meadow.

B. Sampling Strategy and Data Collection

Field survey data were obtained from both permanent and random sampling sites (see Fig. 1). Permanent sampling sites

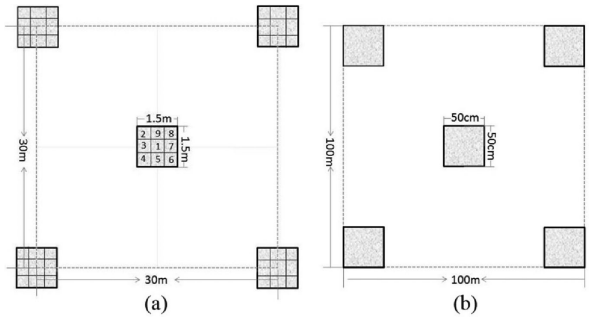

Fig. 2. (a) Permanent site, distribution of five quadrats (1.5 × 1.5 m) in each plot (30 × 30 m). Each plot consists of nine quadrats (0.5 × 0.5 m), the quadrats identification number (1–9) was the order that used to sample grass each time in each of year, e.g., quadrat 1 was used the first time and quadrat 2 in second time of the same year, etc. (b) Random plot, distribution of 5 quadrats (0.5 × 0.5 m) in each plot of 100 × 100 m. constant.

were designed in Yangji Community with 272.26×10^4 ha covered in Gannan region. Random sampling sites were established throughout the Gannan region. For all sampling sites, plots were selected based on two criteria: 1) with relative uniformity and spatial representativeness of grassland growth status; and 2) the area of the sampling sites should reflect grassland status within one MODIS pixel. Besides, the random plot site should ensure a 5 km horizontal distance and homogeneity between plots in both vegetation and land use.

Totally 13 permanent sites were established inside Yangji Community. In each permanent site, a 30 × 30 m plot was established for data acquisition. In each plot, five quadrats (1.5 × 1.5 m) were designed [see Fig. 2(a)]. The entire plot was reflected by central point and other four corner quadrats. In random sampling site a 100 × 100 m plot was set up for ground sampling. In each plot, five quadrats (0.5 × 0.5 m) were used, one for central point and others for corner point [see Fig. 2(b)]. A total of 27 field investigations were conducted during grassland growth season from 2011 to 2016, including 1325 permanent quadrats and 828 random quadrats (see Table I). The whole observed grassland AGB data were used to construct and analyze the biomass estimation model. In each quadrat, above ground grass was cut using shears with nonplant material removed. Then samples were dried in the lab at 64 °C, grass AGB data were recorded until the weight remained constant.

C. MODIS Vegetation Data Preprocess

MOD13Q1 vegetation indices (NDVI and EVI) were downloaded from the United States National Aeronautics and Space Administration (images orbit number h26v05), Totally 27 images with resolution of 250 m were obtained during 2011 to 2016. Map projection of MOD13Q1 NDVI and EVI were transformed and registered to Albers by MODIS reprojection tool, the spatial resolution resampled to 250 m.

D. DEM, Soil, and Meteorological Data Preprocess

DEM data were obtained by shuttle radar topography mission images (version V004),[1] with 90 m spatial resolution and

TABLE I
DATA BETWEEN MODIS IMAGES AND FIELD MEASUREMENTS IN PERMANENT/RANDOM PLOT

Date of MODIS	Date of measurement	Type of site	Number of plots	Number of quadrats
2011.07.29-08.13 2011.08.14-08.28	2011.08.06-08.24	random	66	198
2012.08.30-09.13	2012.09.12-09.13	permanent	5	25
2013.08.30-09.14	2013.09.12-09.13	permanent	13	65
2014.05.26-06.10	2014.05.30-05.31	permanent	13	65
2014.06.11-06.26	2014.06.14-06.16	permanent	13	65
2014.06.27-07.12	2014.06.28-06.29	permanent	13	65
2014.07.13-07.28	2014.07.11-07.13	permanent	13	65
2014.07.13-07.28	2014.07.26-07.28	permanent	13	65
2014.08.14-08.29	2014.08.14-08.15	permanent	13	65
2014.08.30-09.14	2014.09.01-09.02	permanent	13	65
2014.09.15-09.30	2014.09.26-09.28	permanent	13	65
2014.10.17-11.01	2014.10.20-10.22	permanent	13	65
2015.05.10-05.25	2015.05.20-05.22	permanent	13	65
2015.07.13-07.28	2015.07.14-07.15	permanent	13	65
2015.07.13-07.28	2015.07.24-07.25	permanent	13	65
2015.07.13-07.28	2015.07.20-07.25	random	49	245
2015.07.29-08.13	2015.08.10-08.11	permanent	13	65
2015.08.14-08.29	2015.08.20-08.23	permanent	13	65
2015.08.30-09.14	2015.09.11-09.13	permanent	13	65
2015.09.15-09.30	2015.09.19-09.23	random	25	125
2015.10.01-10.16	2015.10.10-10.11	permanent	13	65
2015.10.17-11.01	2015.10.20-10.22	permanent	13	65
2016.07.13-07.28	2016.07.21-07.26	random	28	140
2016.07.13-07.28	2016.07.28-07.29	permanent	13	65
2016.08.14-08.29	2016.08.20-08.25	random	21	105
2016.08.14-08.29	2016.08.20-08.25	permanent	13	65
2016.09.15-09.30	2016.09.24-09.26	random	3	15

Geo-TIFF format. The slope, aspect, and topographic position index (TPI) were calculated based on DEM. Soil data were downloaded from.[2] Both sand and clay concentrations in surface soil (0–30 cm) and bottom soil (30–60 cm) were downloaded, here represented as clay1, sand1, clay2, sand2. Meteorological data were downloaded from the dataset of daily surface observation value of China (V3.0).[3] Daily temperature and precipitation data were downloaded from 38 meteorological stations and surrounding areas in Gannan region from 2011 to 2016 (see Fig. 3). In each station, the monthly mean air temperature and cumulative precipitation were calculated. Anusplin software package was used to interpolate the station-specific data with thin plate smoothing spline interpolation method [29].

For further processing, projections of DEM, slope, aspect, TPI, soil, and selected meteorological data were defined as Albers. Value of each factor and corresponded observation data were obtained by ArcGIS software. Modeling and accuracy evaluation were processed in MATLAB.

E. Grassland AGB Estimation Models

The grassland AGB estimation models included univariate parameter models, multivariate parameter, and multivariate nonparameter models. The univariate parameter models include linear, exponential, logarithmic, and power separate regression models. These models were constructed based on 12 variables [topography factor: DEM, slope (S), aspect (A) and TPI; soil factor: sand1 (S1), clay1 (C1), sand2 (S2) and clay2 (C2);

[1]Online. [Available]: http://srtm.csi.cgiar.org/

[2]Online. [Available]: http://globalchange.bnu.edu.cn/research/soil

[3]Online. [Available]: http://cdc.cma.gov.cn/

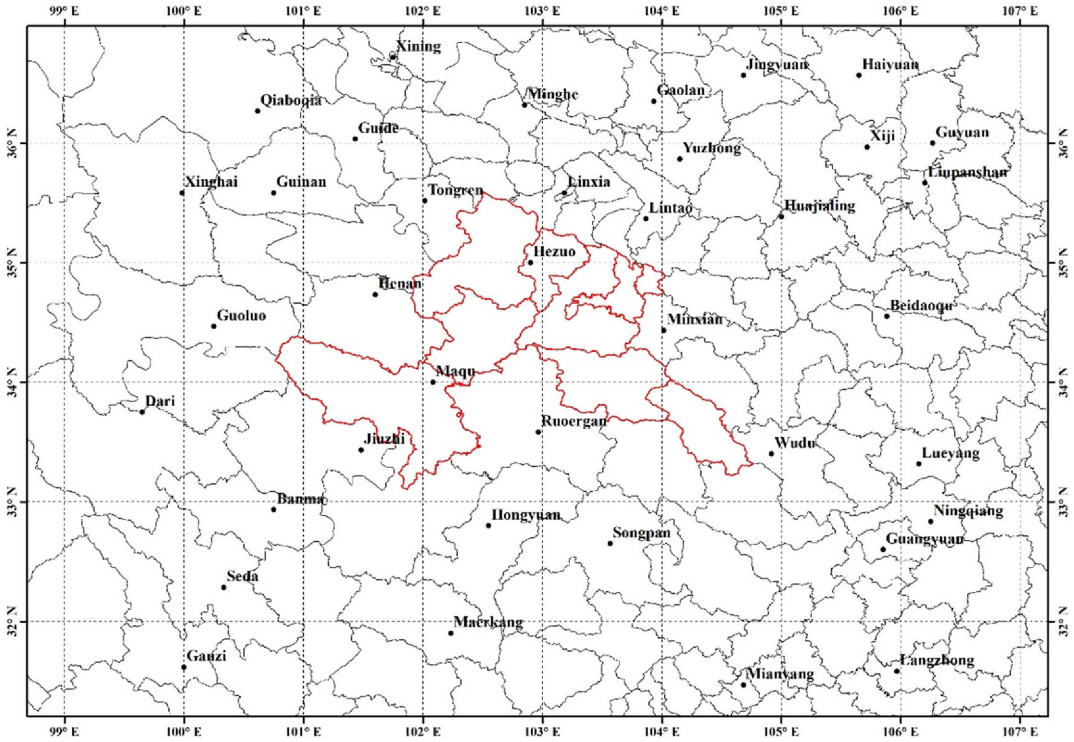

Fig. 3. Locations of the meteorological stations in Gannan region and surrounding area.

meteorological factor: monthly average air temperature (T) and cumulative precipitation (P); MODIS vegetation index: NDVI and EVI and measured grassland AGB data].

Multivariate parameter models included linear, logarithmic, power, and reciprocal multivariate regression models (1)–(4). Variables of multivariate parameter models were selected by calculating their correlations with grassland AGB. The multivariate parameter models were expressed as follows:

$$y = \beta_1 + \beta_2 x_1 + \beta_3 x_2 + \cdots + \beta_{i+1} x_i + u_i \tag{1}$$

$$y = \beta_1 + \beta_2 \ln x_1 + \beta_3 \ln x_2 + \cdots + \beta_{i+1} \ln x_i + u_i \tag{2}$$

$$y = \mathrm{A} x_1^{\beta_1} x_2^{\beta_2} \ldots x_i^{\beta_i} e^{u_i} \tag{3}$$

$$y = \beta_1 + \beta_2 (1/x_1) + \beta_3 (1/x_2) + \cdots + \beta_{i+1} (1/x_i) + u_i \tag{4}$$

where y represented grassland AGB; $x_1, x_2, \ldots, x_i$ were variable; $\beta_1, \beta_2, \ldots \beta_{i+1}$ were model-fitting coefficients; and u_i represented error term.

Multivariate nonparameter models employed in this study were BP-ANN, SVM, and RF models. Variables of these models were in consistent with multivariate parameter models. BP-ANN referred to a multilayer network structure consisting of an input layer, an output layer, and one or more hidden layers. The Levenberg–Marquardt function algorithm was selected for ANN training in this study. The number of neurons and hidden layers were determined based on a trial-and-error process. In this study, BP-ANN model was constructed and validated with MATLAB Neural Network toolbox. SVM was a supervised learning model with associated learning algorithms, and was constructed by a set of hyperplanes in high- or infinite-dimensional space, and these could be employed for classification, regression, and other tasks. Generally, the higher the functional margin, the lower the generalization error of the classifier and regression. In this study, the radial basis function was used as the kernel function, and the optimal cost and gamma values were obtained using the "Libsvm" package [41] in MATLAB. RF approach applies a set of decision trees to improve prediction accuracy, and the RF algorithm is based on the classification tree algorithm. RF regression used bootstrap sampling, and each bootstrap sample was employed to construct a decision tree. The training samples were constantly selected to minimize the sum of the squared residuals until a complete tree was formed. Multiple decision trees were formed, and voting was used to obtain the final prediction. The model was established and validated using the RF function in the "RF_MexStandalone-v0.02" package within MATLAB.

F. Model Accuracy and Stability Evaluation

Performance of above-mentioned grassland AGB estimation models were evaluated with 10-fold cross-validation method. All data were divided into ten groups, each group contained an approximate equal number of samples for cross validation. In each evaluation, 10% of the samples (1/10 of the total samples) were used as a test set, and the remainder as training set (except for the case of BP-ANN, 10% of samples consist test set, another 10% as validation set, and remaining 80% as training set). For each dataset, the value of RMSE and R^2 were calculated. Process was repeated 10 times until each group had been employed as both a test set and a training set. Mean RMSE and R^2 were used to reflect model's performance obtained in the 10 runs. The higher

TABLE II
DESCRIPTIVE STATISTICS OF MEASURED GRASSLAND AGB DURING GROWTH SEASON OF 2011–2016 IN STUDY AREA ($N = 2053$)

Study Area	Grassland AGB (kg/ha)				
	Maximum	Minimum	Average	Std	CV
Xiahe	4875.20	424.80	2020.18	945.02	0.47
Luqu	5335.20	728.00	2584.95	1350.27	0.52
Maqu	9394.00	359.20	2800.42	1509.86	0.54
Hezuo	6395.20	517.67	2115.62	1273.05	0.60
Diebu	2178.76	178.00	1067.83	778.48	0.73
Lintan	2756.00	423.20	1570.82	862.24	0.55
Zhuoni	5335.60	423.60	2259.97	1170.61	0.52
Gannan	9394.00	359.20	2389.54	1284.41	0.54

Note: Std depicts standard deviation, CV depicts coefficient of variation.

R^2 value and the smaller RMSE value, the higher the precision. Standard deviation (SD) of RMSE and R^2 of test set (denoted by $\mathrm{SD}_{\mathrm{RMSE}}$ and SD_{R^2}) were used to reflect model's stability, the closer SD to 0, the higher the stability of model. RMSE and SD were calculated as follows:

$$\mathrm{RMSE} = \sqrt{\frac{\sum_{i=1}^{n} \left(\mathrm{Biomass}_i - f_{\mathrm{Biomass}}(i)\right)^2}{n}} \tag{5}$$

$$\mathrm{SD} = \sqrt{\sum_{i=1}^{n} (x_i - \bar{x})^2 / N} \tag{6}$$

where $\mathrm{Biomass}_i$ represented the ith observed grassland biomass, $f_{\mathrm{Biomass}}(i)$ represented the ith grassland biomass estimated by model, n represented the plots of the test set, x_i was repeated RMSE and R^2 of the test set, $\bar{x}$ was the average of x_i, and N was the number of modeling and validation repetition.

III. RESULTS

A. Characteristics of Observed Grassland AGB in Gannan Region

The measured grassland AGB in Gannan region during 2011 to 2016 was shown in Table II. There was a considerable difference in grassland AGB in a total of 2053 sampling quadrats during grass growing season. The average grassland AGB ranged from 1067.83 to 2800.42 kg/ha and coefficient variation (CV) ranged from 0.47 to 0.73. The maximum and minimum biomass differed greatly, with 9394 and 178 kg/ha, respectively. The largest average biomass showed in Maqu, with AGB and CV of 2800.42 kg/ha and 0.54, respectively. The lowest showed in Diebu (1067.83 kg/ha and 0.73, respectively). The average AGB in other countries followed by Luqu, Zhuoni, Hezuo, Xiahe, and Lintan, ranged from 1570.82 to 2584.95 kg/ha, and CV within 0.47–0.60. For entire study area, the average AGB and CV were 2389.54 kg/ha and 0.54, respectively.

B. Univariate Parameter Models

Results of accuracy evaluation, through 10-fold cross validation for univariate parameter grassland AGB models were shown in Table III. In four types of univariate models based on MODIS vegetation indices exhibited the best performance, with R^2 in a range of 0.32–0.35, and RMSE ranging from 876.65 to 906.64 kg/ha. These were followed by atmosphere, with R^2 of 0.11–0.23, RMSE of 951.56–1039.65 kg/ha. Univariate models based on soil and topography showed low accuracy, R^2 was lower than 0.1, and RMSE ranged within 1070.76–1085.08 kg/ha.

According to the accuracy evaluation, the parameter estimation of each univariate parameter model and the results of *T* and *F* test are shown in Table IV. Univariate parameter AGB estimation model is shown in Table V. Variables of DEM, *T*, *P*, TPI, Clay2, EVI, and NDVI passed the significant test ($P < 0.05$). The optimum models based on MODIS EVI and NDVI were exponential, with R^2 of 0.35 (both) and RMSE of 876.65 and 877.87 kg/ha, respectively, followed by exponential model based on precipitation and logarithmic model based on temperature. Linear models based on DEM, *S, A*, TPI, Clay1, and Clay2 exhibited best performance. Logarithm model based on Sand1 and Sand2 performed best. However, models based on topography and soil factors showed low R^2 and high RMSE.

TABLE III
VALIDATION RESULTS THROUGH 10-FOLD CROSS VALIDATION FOR UNIVARIATE PARAMETER AGB ESTIMATION MODEL

Variable	Linear		Exponential		Logarithm		Power	
	R^2	RMSE	R^2	RMSE	R^2	RMSE	R^2	RMSE
DEM	0.06	1050.96	0.06	1051.22	0.06	1051.37	0.06	1051.06
T	0.12	1031.37	0.11	1039.65	0.14	1021.02	0.17	1020.35
P	0.23	960.49	0.23	960.09	0.22	963.35	0.23	951.56
S	0.01	1078.14	0.01	1078.36	-	-	-	-
A	0.01	1080.72	0.01	1080.66	-	-	0.01	1078.81
TPI	0.04	1075.09	0.04	1075.27	0.05	1076.80	0.05	1077.71
Clay1	0.03	1078.44	0.03	1078.74	0.03	1080.17	0.03	1080.27
Clay2	0.04	1070.76	0.04	1071.23	0.04	1073.79	0.04	1074.53
Sand1	0.04	1085.03	0.04	1085.08	0.04	1084.67	0.04	1084.67
Sand2	0.08	1073.05	0.08	1073.35	0.07	1071.73	0.07	1071.81
EVI	0.33	896.35	0.35	876.65	0.32	906.64	0.35	887.95
NDVI	0.34	880.11	0.35	877.87	0.33	890.13	0.35	877.75

Note: *T* and *P* represent monthly average air temperature and cumulative precipitation, *S*, *A*, and TPI represent slope, aspect, and topographic position index, clay1, sand1, clay2, sand2 represent sand and clay concentrations in surface soil (0–30 cm) and bottom soil (30–60 cm), units of RMSE is kg/ha and the bold fonts represent the best performance in four types of model.

TABLE IV
RESULTS OF MODEL FITTING WITH THE OPTIMUM INVERSION MODELS BASED ON UNIVARIATE FACTOR

Variable	Model	Parameter Estimation and T test			Regression significance test	
		Parameter	Estimated value	T	R^2	F
DEM	Linear	A	0.991	3.812**	0.049	14.531**
		B	-1127.971	-1.320		
T	Logarithm	A	1.484	7.7**	0.174	59.286**
		B	1.631	1.095		
P	Exponential	A	0.730	8.498**	0.204	72.213**
		B	13.536	1.728		
S	Linear	A	13.341	1.152	0.005	1.328
		B	2068.264	26.140*		
A	Linear	A	1.122×10-4	0.339	0.001	0.115
		B	1802.909	15.699**		
TPI	Linear	A	-157.196	-2.509*	0.015	4.238*
		B	2751.544	8.803**		
Clay1	Linear	A	-34.741	-1.344	0.006	1.807
		B	2695.793	6.242**		
Clay2	Linear	A	-34.798	-2.479*	0.021	6.145*
		B	2819.965	9.765**		
Sand1	Logarithm	A	87.088	0.226	8.878×10-6	0.051
		B	1821.952	1.372		
Sand2	Logarithm	A	808.205	2.622*	0.002	0.873
		B	-585.783	-0.566		
EVI	Exponential	A	3.295	12.489**	0.356	155.965**
		B	372.049	7.655**		
NDVI	Exponential	A	3.782	12.489**	0.343	147.337**
		B	124.169	4.472**		

Note: *represent $p<0.05$; **represent $p < 0.001$; *a* and *b* represent the constant and exponential term of the models, respectively; *T* and *F* are the significant values according to the *T* and *F* tests. *T* and *P* represent monthly average air temperature and cumulative precipitation, *S, A*, and TPI represent slope, aspect and topographic position index, clay1, sand1, clay2, sand2 represent the sand and clay concentrations in surface soil (0–30 cm) and bottom soil (30–60 cm).

TABLE V
BEST FITTED MODELS CONSTRUCTED BASED ON UNIVARIATE FACTOR

Factor	Variable	Formula	R^2
Topography	DEM	y=0.991x-1127.971	0.049
	TPI	y= - 157.196x+2751.544	0.015
Soil	Clay2	y= - 34.798x+2819.965	0.021
Atmosphere	T	$y=1.484x^{1.631}$	0.174
	P	$y=0.730x^{13.536}$	0.204
Vegetation indices	EVI	$y=3.295e^{372.049x}$	0.356
	NDVI	$y=3.782e^{124.169x}$	0.353

Note: *T* and *P* represent monthly average air temperature and cumulative precipitation, TPI represent topographic position index, and clay2 represent the clay concentrations in bottom soil (30–60 cm).

TABLE VI
ACCURACY ASSESSMENT OF THE DIFFERENT MULTIVARIATE PARAMETER MODELS USING THE 10-FOLD CROSS-VALIDATION METHOD

Combination of different factors	Variables	Model	Test set		Train set	
			R^2	RMSE	R^2	RMSE
topography, atmosphere, soil and MODIS vegetation indices	DEM, TPI, T, P, Clay2, EVI	Linear	0.41	825.69	0.42	840.50
		Logarithm	0.41	828.26	0.42	833.88
		Power	**0.44**	**809.39**	**0.44**	**817.48**
		Reciprocal	0.41	831.88	0.41	843.00

Note: units of RMSE is kg/ha; *T* and *P* represent monthly average air temperature and cumulative precipitation, TPI represent topographic position index, clay2 represent the clay concentrations in bottom soil (30–60 cm), blod fonts represent the best performance in four types of model.

TABLE VII
BEST FITTED MODELS CONSTRUCTED BASED ON MULTIVARIATE

Formula	R^2	F
$y=-5.33\times103+0.89DEM+17.45TPI+0.59T-53.75P+13.75Clay2+4.04\times10^3EVI$	0.42	128.39**
$y=9.94\times10^3-1.12\times10^7/DEM-2.66\times10^5/Tpi-3.52\times10^5/temp-69.47/prec-4.39\times10^3/Clay2-602.31/EVI$	0.40	127.35**
$y=-3.71\times10^4+3.24\times10^3\ln(DEM)+2.21\times10^3\ln(TPI)+459.39\ln(T)-96.63\ln(P)+273.67\ln(Clay2)+1.65\times10^3\ln(EVI)$	0.42	129.23**
$y=3.16\times10^{-10}DEM^{2.64}Tpi^{1.60}temp^{0.14}prec^{-0.0072}Clay2^{0.05}EVI^{0.76}$	0.44	162.40**

Note: *represent $p < 0.05$, **represent $p < 0.01$; *T* and *P* represent monthly average air temperature and cumulative precipitation, TPI represent topographic position index, clay2 represent the clay concentrations in bottom soil (30–60 cm).

C. Multivariate Parameter Models

The accuracy evaluation (through 10-fold cross validation) for multivariate parameter models based on six variables (significant correlated with grass AGB in Section III-B) and 2153 sample data in Gannan region were shown in Table VI. Multivariate power model exhibited the best performance, with R^2 and RMSE of 0.44 and 817.48 kg/ha, respectively (see Table VI, bold words). Followed by multivariate linear and logarithmic models, with R^2 of 0.42, and RMSE of 833.88–840.50 kg/ha. The accuracy of multivariate reciprocal model exhibited the worst, with R^2 of 0.41 and RMSE of 843.00 kg/ha. According to parameter estimation for each multivariate model and *F* test (see Table VII), the multivariate AGB estimation models were obtained, as shown in Table VII. All models passed the F test with significant level of $P < 0.001$. Among all the multivariate models, the power model has the highest R^2 (0.44), and reciprocal model has the lowest R^2 (0.41).

TABLE VIII
BEST FITTED MODELS CONSTRUCTED BASED ON MULTIVARIATE

Factors	Variables	Model	Training set		Test set	
			R^2	RMSE	R^2	RMSE
Topography, atmosphere, soil and vegetation indices	DEM,TPI,T,P, Clay2, EVI	BP-ANN	0.56	756.46	0.56	745.33
		SVM	0.75	543.90	0.70	694.59
		RF	0.90	377.66	0.78	601.26

Note: *T* and *P* represent monthly average air temperature and cumulative precipitation, TPI represent topographic position index, and clay2 represent the clay concentrations in bottom soil (30–60 cm).

TABLE IX
STABILITY OF UNIVARIATE PARAMETRIC MODELS IN PREDICTION OF GRASSLAND AGB

Factor	Variable	Model	SD_{R^2}	SD_{RMSE} (kg/ha)
Topography	DEM	Linear	0.048	135.463
	TPI	Linear	0.074	113.983
Atmosphere	T	Power	0.099	121.653
	P	Power	0.122	144.148
Soil	Clay2	Linear	0.041	107.620
Vegetation index	EVI	Exponential	0.149	159.729
	NDVI	Exponential	0.134	144.602

Note: *T* and *P* represent monthly average air temperature and cumulative precipitation, TPI represent topographic position index, clay2 represent the clay concentrations in bottom soil (30–60cm), and SD_{R^2} and SD_{RMSE} represent standard deviation of RMSE and R^2.

D. Multivariate Nonparameter Models

The accuracy evaluation through 10-fold cross validation for BP-ANN, SVM, and RF models is shown in Table VIII. In three types of machine learning methods, RF model exhibited best performance, with R^2 of 0.78, and RMSE of 601.26 kg/ha. The performance followed by SVM model, with R^2 and RMSE of 0.70 and 694.59 kg/ha, respectively. BP-ANN model showed the lowest performance with R^2 and RMSE of 0.56 and 745.33 kg/ha.

E. Stability of Different Models

Stability of univariate parametric models was showed considerable variety. These models with high accuracy did not have high stability (see Table IX). The SD_{R^2} and SD_{RMSE} for EVI and NDVI showed lower stability while a higher accuracy. Among all the models, the stability of optimum model based on Clay2 was the highest, with SD_{R^2} of 0.041 and SD_{RMSE} of 107.620 kg/ha; and those based on EVI exhibited lowest, with SD_{R^2} and SD_{RMSE} of 0.149 and 159.729 kg/ha.

The stability of multivariate models was showed in Table X. For parametric models, the power model showed highest stability, with SD_{R^2} of 0.095 and SD_{RMSE} of 117.262 kg/ha. For nonparametric models, the model based on RF algorithm exhibited best stability, with SD_{R^2} of 0.074 and SD_{RMSE} of 64.061 kg/ha. Among three types of grassland AGB model, the multivariate non-parametric models (based on machine learning algorithm) exhibited highest stability, followed by multivariate parametric models. Univariate parametric models showed lowest stability.

TABLE X
PERFORMANCE OF MULTIVARIATE PARAMETRIC MODELS IN THE PREDICTION OF GRASSLAND AGB

Factors	Type	Model	$SD_R{}^2$	SD_{RMSE} (kg/ha)
DEM, TPI, T, P, Clay2, EVI	Parametric	Linear	0.127	131.127
		Logarithm	0.102	118.520
		Power	0.095	117.262
		Reciprocal	0.117	125.343
	Non-parametric	BP-ANN	0.090	105.593
		SVM	0.074	66.131
		RF	0.074	64.061

Note: *T* and *P* represent monthly average air temperature and cumulative precipitation, TPI represent topographic position index, and clay2 represent the clay concentrations in bottom soil (30–60 cm).

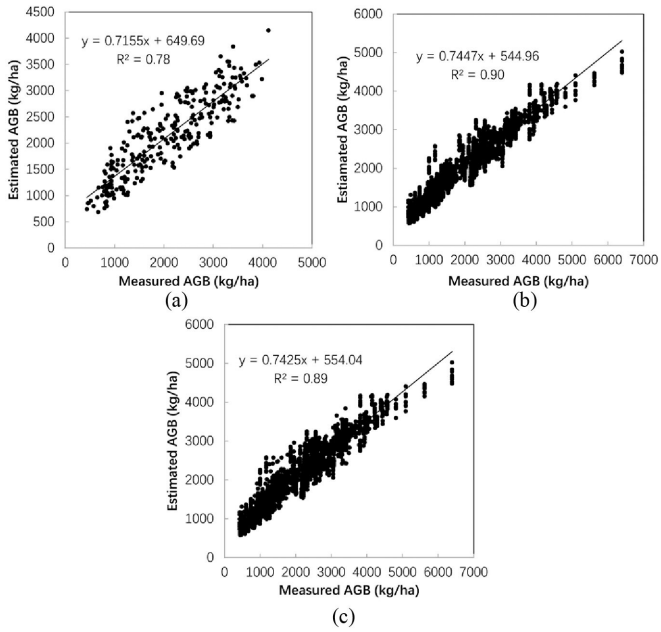

Fig. 4. Simulated results of grassland AGB based on RF algorithm test set data. (a) Test dataset. (b) Training dataset. (c) All dataset.

Combined with the accuracy assessment (see Table VIII), RF model was the most suitable for reflecting inversion of grassland AGB in study region. This model could account for 89.41% of the variation in grassland AGB in growing season (see Fig. 4).

IV. DISCUSSION

A. Influence of Various Factors on Grassland AGB in Gannan Region

Univariate parameter model is one of the most simple and commonly applied model in grassland AGB estimation via remote sensing approach. Studies on estimating grassland AGB based on MODIS vegetation indices have made great achievements [20], [21], [25], [27], [42]. Furthermore, previous studies indicated that grassland AGB has a significant correlation with temperature and precipitation [15], [20], [43], [44]. The soil texture (including sand and clay content) also deeply influenced the grassland AGB [45]. Liang *et al.* and Yang *et al.* (2017) indicated that grassland AGB was not only correlated with remote sensing vegetation indices but also correlated with the grass biophysics, topography and geographical location (with correlation coefficient of 0.185–0.425) [24], [28].

This study aimed to explore the best method for grassland AGB estimation, the MODIS vegetation indices and ten factors (DEM, S, A, TPI, Clay1, Sand1, Clay2, Sand2, T, and P) are considered. Generally, the parametric models based on univariate have lower accuracy and poor stability. Univariate grassland AGB estimation models based on MODIS vegetation indices accounted for 35.3%–35.6% of the variation in AGB, while single factor accounted for only 1.5%–36.3% of the variation in AGB during the growing season. The $SD_R{}^2$ and SD_{RMSE} of all univariate models ranged from 0.041–0.149 and 97.479 kg/ha–159.729 kg/ha, respectively. These results were similar to studies of Liang *et al.*, (2016) and Yang *et al.*, (2017) in Three-River Headwaters Region.

B. Performance of Three Types of AGB Estimation Models

Compared with univariate parameter models, multivariate parameter models showed higher performance. Lv indicated that the accuracy of grassland AGB parameter model (based on combination of MODIS EVI, effective precipitation, temperature, and dryness) was higher than MODIS NDVI or EVI alone, with R^2 increased 0.065–0.090, precision increased 2.80%–4.09% in Xilingguole grassland [44]. Han constructed the multivariate parameter AGB model based on Landsat TM image band, vegetation indices, slope, aspect and elevation in Yongding river basin. His study indicated that this model exhibited higher performance than the model constructed by TM NDVI and RVI, respectively, with R^2 increased 0.098–0.150, precision increased 7.37%–9.74% [46]. Diouf *et al.* studied the semi-arid grassland in Sahel region, their research indicated a combined photosynthetic radiation and meteorological data model performed better ($R^2 = 0.69$ and RMSE = 483 kg DW/ha) than univariate model of photosynthetic radiation or meteorological data ($R^2 = 0.63$ and 0.55 and RMSE = 550 kg DW/ha and 585 kg DW/ha, respectively) [45]. Liang *et al.* studied the alpine meadow grassland AGB inversion model in the Three-River Headwaters Region, research indicated that a multivariate model showed decreased RMSE by 14.5% as compared with the optimum univariate model [24]. Yang *et al.* used BP-ANN constructed an AGB model based on five variables and showed that BP ANN achieved better results than traditional multi-factor regression models (R^2: 0.75–0.85 versus 0.40–0.64, RMSE: 355–462 versus 537–689 kg DW/ha) [28].

This study showed that accuracy of AGB estimation model based on MODIS vegetation index can be greatly improved when considering various factors crucial for grass growth, these results are in consistent with previous studies [23], [24], [29]. Performance of multivariate nonparameter models are highest among three types of AGB estimation models, followed by multivariate parameter models and univariate parameter models perform poorly (see Table XI). Compared with the univariate/multivariate parameter models, the RMSE of RF model decreases 26.45%–44.27%. Meanwhile, the models can explain

TABLE XI
STABILITY OF UNIVARIATE PARAMETRIC MODELS IN PREDICTION OF GRASSLAND AGB

Combination	Variable	Model	Training set			
			R^2	RMSE (kg/ha)	$SD_R{}^2$	SD_{RMSE} (kg/ha)
1	DEM、TPI、T、P、Clay2、	Parameter	0.44	809.39	0.095	117.262
		Non-parameter	0.78	601.26	0.074	64.061
2	DEM、TPI、T、P、EVI	Parameter	0.41	819.75	0.175	111.037
		Non-parameter	0.50	764.02	0.158	102.169
3	T、P、EVI	Parameter	0.39	834.62	0.168	106.352
		Non-parameter	0.45	796.17	0.145	104.764

Note: Combination represents different combinations: 1, Topography, Atmosphere, soil, and MODIS vegetation index; 2, the combination of Topography, Atmosphere and MODIS vegetation index; 3, Atmosphere and MODIS vegetation index. *T* and *P* represent monthly average temperature and cumulative precipitation, TPI represent topographic position index, and clay2 represent the clay concentrations in bottom soil (30–60 cm), respectively.

89.41% of the variation in AGB during grass growing season in Gannan area (see Fig. 4).

C. Comparision of Optimum Parameter/Nonparameter Models Based on Different Variable Combinations

To further confirm the performance of multivariate AGB models, the same 2053 samples and 10-fold cross validation method were used to construct RF and multivariate power models based on different combinations (Topography, Atmosphere, soil, and MODIS EVI; for each time one type of factor removed, which had lower correlation with grassland AGB than others). Results showed that nonparameter models performed better than corresponding parameter models in accuracy, with 0.45–0.78 versus 0.39–0.44 for R^2, 601.26–796.17 kg/ha versus 809.39–834.62 kg/ha for RMSE on test dataset. Meanwhile, the value of SD for R^2 was similar in nonparameter and corresponding parameter models. However, the model SD_{RMSE} was lower in non-parameter models, with 106.352 kg/ha–117.262 kg/ha vs. 64.061 kg/ha–104.764 kg/ha. With number of variables decreasing, SD_{RMSE} of parameter models presented a decreasing trend. However, in RF models, SD for R^2 and RMSE presented an increasing trend.

D. Factors Affecting the Accuracy of Grassland AGB Estimation via Remote Sensing Approach

The optimum AGB estimation model was investigated by comparing univariate parameter models, multivariate parameter/nonparameter models. However, there is still some limitations and uncertainty for these inversion models. The representativeness of the ground sampling plot [24] and temporal matching between ground sampling sites and remote sensing data are the main cause of the uncertainty [25], [28]. Compare with parametric models, RF model is a data-driven method. The RF model can automatically retrieve and interpret data, moreover, the algorithm is flexible. With the increase of input dataset, the estimation results of models are improved correspondingly [41], [46], [47]. RF model composes of a large sample decision tree based on high-dimensional data training and has a strong tolerance for data error [48], [49]. However, it is difficult to train RF model effectively with small samples dataset, because it requires a large amount of marked and ground measured data, and usually a certain of programming basis is also required [47], [50]. Besides, this kind of model involves many independent variables, and some variables (such as atmosphere factors) have large errors in spatial quantization. Therefore, the model still has some limitations and uncertainties [15], [51].

Although RF model has higher retrieval accuracy, there are still unavoidable factors that affect model accuracy. First, spatiotemporal inconsistency exists between field-measured data and satellite data. MODIS images are more susceptible to clouds over the Tibet plateau in summer, the approximate monthly MODIS product is generated by averaging two MODIS products over 16-day intervals. This phenomenon minimizes the impacts from bad pixels and cloud pixels. Therefore, to ensure a large amount of valid data to train the RF model, we used the monthly MODIS data to match the field-measured data. The representation of the sample plots was not perfect because the study area had complicated topography. When grassland tends to degenerate, other surface features (i.e., bare soil and rock) in the MODIS pixel had some influence on vegetation indices (e.g., NDVI and EVI), which were used in establishing models. Hence, we will consider using high spatiotemporal resolution images in future research. Second, the uneven distribution of the sample plots produced some errors and uncertainty in construction models. Most of the sample plots were distributed in the eastern part of the Tibet Plateau, while the number of sample plots in the middle and western regions was limited due to restrictions of road access and altitude. Third, due to the uneven distribution of meteorological stations on the Tibet Plateau, there were some errors in the spatial interpolation of meteorological data.

V. CONCLUSION

Based on the factors significantly correlated with grassland AGB in Gannan region, this study examined univariate parametric and multivariate parametric/nonparametric AGB inversion models, then evaluated their accuracy and stability. The main conclusions are as follows:

1) six out of ten factors (DEM, TPI, *T, P*, Clay2 and EVI) exert a significant effect on grassland AGB in study area;
2) the accuracy and stability of grassland AGB estimation model can be improved using multivariate method, especially multivariate nonparameter models;
3) considering the accuracy and stability, in alpine grassland the multivariate nonparameter model based on RF algorithm (variables including DEM, TPI, *T, P*, Clay2 and EVI) is selected as the AGB monitoring model, the RMSE of RF model decreased 26.45%–44.27% than other models.

Meanwhile, RF model can explain 89.41% of the variation of grassland AGB during grass growing season in Gannan region.

REFERENCES

[1] J. Adams, H. Faure, L. Fauredenard, and J. McGlade, "Increases in terrestrial carbon storage from the last glacial maximum to the present," *Nature*, vol. 348, no. 6303, pp. 711–714, Dec. 1990.

[2] R. White, S. Murray, M. Rohweder, R. White, S. Murray, and M. Rohweder, "Pilot analysis of global ecosystems: Grassland ecosystems," *World Resour. Inst.*, vol. 4, no. 6, 2000, Art. no. 275.

[3] J. Scurlock and D. Hall, "The global carbon sink: A grassland perspective," *Global Change Biol.*, vol. 4, no. 2, pp. 229–233, 1998.

[4] A. Hopkins, "Relevance and functionality of semi-natural grassland in Europe–status quo and future prospective," in *Proc. Int. Workshop Salvere*, Jan. 2009, pp. 9–14.

[5] W. Lauenroth, H. Hunt, D. Swift, and J. Singh, "Estimating aboveground net primary production in grasslands: A simulation approach," *Ecol. Model.*, vol. 33, no. 2, pp. 297–314, Oct. 1986.

[6] J. Soussana, P. Loiseau, and N. Vuichard, "Carbon cycling and sequestration opportunities in temperate grasslands," *Soil Use Manage.*, vol. 20, no. 2, pp. 219–230, Jun. 2004,

[7] J. Scurlock, K. Johnson, and R. Olson, "Estimating net primary productivity from grassland biomass dynamics measurements," *Global Change Biol.*, vol. 8, no. 8, pp. 736–753, Jul. 2002.

[8] M. Thurner *et al.*, "Carbon stock and density of northern boreal and temperate forests," *Global Ecol. Biogeography*, vol. 23, no. 3, pp. 297–310, Mar. 2014.

[9] Y. Dong, T. Lei, S. Li, C. Yuan, S. Zhou, and X. Yang, "Effects of rye grass coverage on soil loss from loess slopes," *Int. Soil Water Conservation Res.*, vol. 3, no. 3, pp. 170–182, Sep. 2015.

[10] J. Hou, H. Wang, B. Fu, L. Zhu, Y. Wang, and Z. Li, "Effects of plant diversity on soil erosion for different vegetation patterns," *Catena*, vol. 147, pp. 632–637. Dec. 2016.

[11] X. Yao, J. Yu, H. Jiang, W. Sun, and Z. Li, "Roles of soil erodibility, rainfall erosivity and land use in affecting soil erosion at the basin scale," *Agric. Water Manage.*, vol. 174, pp. 82–92, Aug. 2016.

[12] J. Gao and Y. Liu, "Determination of land degradation causes in Tongyu County, Northeast China via land cover change detection," *Int. J. Appl. Earth Obs. Geoinformat.*, vol. 12, no. 1, pp. 9–16, Feb. 2010.

[13] P. Wang, X. Deng, and S. Jiang, "Diffused impact of grassland degradation over space: A case study in Qinghai province," *Phys. Chem. Earth Parts A/B/C*, vol. 101, pp. 166–171, 2017.

[14] B. Xu *et al.*, "MODIS-based remote-sensing monitoring of the spatiotemporal patterns of China's grassland vegetation growth," *Int. J. Remote Sens.*, vol. 34, no. 11, pp. 3867–3878. Jun. 2013.

[15] T. Gao *et al.*, "Using MODIS time series data to estimate aboveground biomass and its spatio-temporal variation in Inner Mongolia's grassland between 2001 and 2011," *Int. J. Remote Sens.*, vol. 34, no. 21, pp. 7796–7810. Sep. 2013.

[16] D. Xu and X. Guo, "Some insights on grassland health assessment based on remote sensing," *Sensors*, vol. 15, no. 2, pp. 3070–3089, Jan. 2015.

[17] I. Ali, F. Cawkwell, E. Dwyer, B. Barrett, and S. Green, "Satellite remote sensing of grasslands: From observation to management—A review," *J. Plant Ecol.*, vol. 9, no. 6, pp. 649–671, Feb. 2016.

[18] S. Moreau, R. Bosseno, F. Xing, and B. Frédéric, "Assessing the biomass dynamics of Andean bofedal, and totora, high-protein wetland grasses from NOAA/AVHRR," *Remote Sens. Environ.*, vol. 85, no. 4, pp. 516–529, Jun. 2003.

[19] J. Nordberg and J. Evertson, "Vegetation index differencing and linear regression for change detection in a Swedish mountain range using Landsat TM; and ETM+; imagery," *Land Degradation Develop.*, vol. 16, no. 2, pp. 139–149, Mar. 2005.

[20] Y. Yang, J. Fang, Y. Pan, and C. Ji, "Aboveground biomass in Tibetan grasslands," *J. Arid Environ.*, vol. 73, no. 1, pp. 91–95, Jan. 2009.

[21] X. Cui, Z. Guo, T. Liang, Y. Shen, X. Liu, and Y. Liu, "Classification management for grassland using MODIS data: A case study in the Gannan region, China," *Int. J. Remote Sens.*, vol. 33, no. 10, pp. 3156–3175, Nov. 2012.

[22] J. Xia *et al.*, "Estimates of grassland biomass and turnover time on the Tibetan Plateau," *Environ. Res. Lett.*, vol. 13, no. 1, Jan. 2018, Art. no. 014020.

[23] F. Yang, J. Wang, P. Chen, Z. Yao, Y. Zhu, and J. Sun, "Comparison of HJ-1A CCD and TM data and for estimating grass LAI and fresh biomass," *Int. J. Remote Sens.*, vol. 16, no. 5, pp. 1000–1023, 2012.

[24] T. Liang *et al.*, "Multi-factor modeling of above-ground biomass in alpine grassland: A case study in the Three-River Headwaters Region, China," *Remote Sens. Environ.*, vol. 186, pp. 164–172, Dec. 2016.

[25] B. Meng *et al.*, "Evaluation of remote sensing inversion error for the above-ground biomass of alpine meadow grassland based on multi-source satellite data," *Remote Sens.*, vol. 9, no. 4, Apr. 2017, Art. no. 372.

[26] R. Li and J. Liu, "Estimating wetland vegetation biomass in the Poyang lake of central China from Landsat ETM data," in *Proc. IEEE Int. Geosci. Remote Sens. Symp.*, vol. 7, pp. 4590–4593, 2004.

[27] B. Xu, X. Yang, W. Tao, Z. Qin, H. Liu, and J. Miao, "Remote sensing monitoring upon the grass production in China," *Acta Ecologica Sin.*, vol. 27, no. 2, pp. 405–413, Feb. 2007.

[28] S. Yang, Q. Feng, T. Liang, B. Liu, W. Zhang, and H. Xie, "Modeling grassland above-ground biomass based on artificial neural network and remote sensing in the Three-River Headwaters Region," *Remote Sens. Environ.*, vol. 204, pp. 448–455, Oct. 2017.

[29] B. Meng *et al.*, "Modeling of alpine grassland cover based on unmanned aerial vehicle technology and multi-factor methods: A case study in the east of Tibetan plateau, China," *Remote Sens.*, vol. 10, no. 2, Feb. 2018, Art. no. 320.

[30] X Quan *et al.*, "A radiative transfer model-based method for the estimation of grassland aboveground biomass," *Int. J. Appl. Earth Obs. Geoinf.*, vol. 54, pp. 159–168, Feb. 2018.

[31] B. He, X. Li, X. Quan, and S. Qiu, "Estimating the aboveground dry biomass of grass by assimilation of retrieved LAI into a crop growth model," *IEEE J. Sel. Topics Appl. Earth Observ. Remote Sens.*, vol. 8, no. 2, pp. 550–561, Feb. 2015.

[32] F. C. Ali, E. Dwyer, and S. Green, "Modeling managed grassland biomass estimation by using multitemporal remote sensing data—A machine learning approach," *IEEE J. Sel. Topics Appl. Earth Observ. Remote Sens.*, vol. 10, no. 7, pp. 3254–3264, Jul. 2017.

[33] F. Li, L. Jiang, X. Wang, X. Zhang, J. Zheng, and Q. Zhao, " Estimating grassland aboveground biomass using multitemporal MODIS data in the West Songnen Plain, China," *J. Appl. Remote Sens.*, vol. 7, no. 1, Jan. 2013, Art. no. 073546.

[34] M. Barrachina, J. Cristóbal, and A. Tulla, "Estimating above-ground biomass on mountain meadows and pastures through remote sensing," *Int. J. Appl. Earth Observ. Geoinf.*, vol. 38, pp. 184–192, Jun. 2015.

[35] B. Reddersen, T. Fricke, and M. Wachendorf, "A multi-sensor approach for predicting biomass of extensively managed grassland," *Comput. Electron. Agric.*, vol. 109, pp. 247–260, Nov. 2014.

[36] A. Diouf *et al.*, "Do agrometeorological data improve optical satellite-based estimations of the herbaceous yield in Sahelian semi-arid ecosystems?" *Remote Sens.*, vol. 8, no. 8, Aug. 2016, Art. no. 668.

[37] Y. Xie, Z. Sha, M. Yu, Y. Bai, and L. Zhang, "A comparison of two models with Landsat data for estimating above ground grassland biomass in Inner Mongolia, China," *Ecol. Model.*, vol. 220, no. 15, pp. 1810–1818, Aug. 2009.

[38] F. Li, Y. Zeng, X. Li, Q. Zhao, and B. Wu, "Remote sensing based monitoring of interannual variations in vegetation activity in China from 1982 to 2009," *Sci. China-Earth Sci.*, vol. 57, no. 8, pp. 1800–1806, May 2014.

[39] B. Zhang, L. Zhang, D. Xie, X. Yin, C. Liu, and L. Guang, "Application of synthetic NDVI time series blended from Landsat and MODIS data for grassland biomass estimation," *Remote Sens.*, vol. 8, no. 1, Dec. 2015, Art. no. 10.

[40] J. Adams, H. Faure, L. Faure-denard, J. McGlade, and F. Woodward, "Increases in terrestrial carbon storage from the Last Glacial Maximum to the present," *Nature*, vol. 348, no. 6303, pp. 711–714, Dec. 1990.

[41] H. Yuan *et al.*, "Retrieving soybean leaf area index from unmanned aerial vehicle hyperspectral remote sensing: Analysis of RF, ANN, and SVM regression models," *Remote Sens.*, vol. 9, no. 4, Mar. 2017, Art. no. 309.

[42] Q. He, "Neural network and its application in IR," Graduate School Library Inf. Sci., Univ. Illinois Urbana-Champaign, Champaign, IL, USA, 2008.

[43] Y. Wang, W Xia, T. Liang, and C. Wang, "Spatial and temporal dynamic changes of net primary product based on MODIS vegetation index in Gannan grassland," *Acta Prataculturae Sin.*, vol. 19, no. 1, pp. 201–210, 2010.

[44] M. Liu, G. Liu, G. Li, D. Wang, and J. Sun, "Relationships of biomass with environmental factors in the grassland area of Hulunbuir, China," *PLoS One.*, vol. 9, no. 7, 2014, Art. no. e102344.

[45] H. Lv, "Study on the method of grassland yield model-a case study of Xilinguole grassland in Inner Mongolia," Ph.D. dissertation, Chin. Acad. Agricultural Sci., Beijing, China, 2010.

[46] M. Dodd, W. Lauenroth, I. Burke, and P. Chapman, "Associations between vegetation patterns and soil texture in the shortgrass steppe," *Plant Ecol.*, vol. 158, no. 2, pp. 127–137, Feb. 2002.

[47] L. Han, "A method of modifying error for non-synchronicity of grass yield remote sensing estimation and measurement," *Int. J. Remote Sens.*, vol. 22, no. 17, pp. 3363–3372, Nov. 2010.
[48] J. Verrelst *et al.*, "Optical remote sensing and the retrieval of terrestrial vegetation bio-geophysical properties – A review," *ISPRS J. Photogramm. Remote Sens.*, vol. 108, pp. 273–290, Oct. 2015.
[49] L. Breiman, "Bagging predictors," *Mach. Learn.*, vol. 24, no. 2, pp. 123–140, 1996.
[50] L. Breiman, "Random forests," *Mach. Learn.*, vol. 45, no. 1, pp. 5–32, Jan. 2001.
[51] I. Ali, F. Cawkwell, S. Green, and N. Dwyer, "Application of statistical and machine learning models for grassland yield estimation based on a hypertemporal satellite remote sensing time series," in *Proc. Geosci. Remote Sens. Symp.*, 2014, pp. 5060–5063.
[52] L. Lehnert *et al.*, "Retrieval of grassland plant coverage on the Tibetan Plateau based on a multi-scale, multi-sensor and multi-method approach," *Remote Sens. Environ.*, vol. 164, pp. 197–207, 2015.

Baoping Meng received the B.S. and Ph.D. degrees from the College of Pastoral Agriculture Science and Technology, Lanzhou University, Lanzhou, China, in 2013 and 2018, respectively.

He is currently a Lecturer with the School of Geographic Sciences, Nantong University, Nantong, China. His research interests include remote sensing of grassland and climate change.

Tiangang Liang received the B.S. degree from the Department of Geology, Lanzhou University, Lanzhou, China, in 1989, the M.S. degree from the Department of Geography, Lanzhou University, in 1992, and the Ph.D. degree from the State Key Laboratory of Arid Agroecology, Lanzhou University, in 1998.

He is a Professor with the College of Pastoral Agriculture Science and Technology, Lanzhou University, and the Director of the Institute of Grassland Remote Sensing and Geographic Information System, Lanzhou University. His research interests include remote sensing and GIS technologies, theories, and applications on grassland ecology and environment.

Shuhua Yi received the B.S. degree from Nanjing University of Information Science & Technology, Nanjing, China, in 1999, the M.S. degree from Chinese Academy of Meteorological Sciences, Beijing, China, in 2002, and the Ph.D. degree from McMaster University, Hamilton, ON, Canada, in 2006.

He is a Professor with the School of Geographic Sciences, Nantong University, Nantong, China, and the Director of the Institute of Fragile Eco-environment, Nantong University. His research interests include application of UAV on studies of fragile region ecosystems, in combination with ground survey, remote sensing, and numerical modeling.

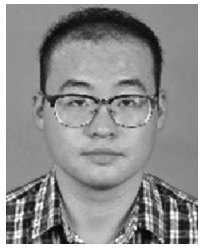

Jianpeng Yin received the B.S. degree from the College of Pastoral Agriculture Science and Technology, Lanzhou University, Lanzhou, China, in 2017. He is currently working toward the M.S. degree in Lanzhou University.

His research interests include remote sensing and GIS of grassland.

Xia Cui received the B.S. degree and Ph.D. degrees from the College of Pastoral Agriculture Science and Technology, Lanzhou University, Lanzhou, China, in 2006 and 2011, respectively.

She is currently a Lecturer with the College of earth and environmental sciences, Lanzhou University. Her research interests include remote sensing of environment and application.

Jing Ge is currently working toward the Ph.D. degree with the College of Pastoral Agriculture Science and Technology, Lanzhou University, Lanzhou, China.

Her research interests include modeling for grassland parameters by remote sensing.

Mengjing Hou is currently working toward the Ph.D. degree with the College of Pastoral Agriculture Science and Technology, Lanzhou University, Lanzhou, China.

His research interests include land cover classification by remote sensing.

Yanyan Lv received the B.S. and Ph.D. degrees from the College of Pastoral Agriculture Science and Technology, Lanzhou University, Lanzhou, China, in 2013 and 2018, respectively.

She is currently a Lecturer with the School of Geographic Sciences, Nantong University, Nantong, China. Her research interests include vegetation changes on grassland in fragile areas.

Yi Sun received the B.S. and Ph.D. degrees from the College of Pastoral Agriculture Science and Technology, Lanzhou University, Lanzhou, China, in 2009 and 2015, respectively.

He is currently a Lecturer with the School of Geographic Sciences, Nantong University, Nantong, China. His research interests include rangeland ecology and management and biodiversity monitoring.